

Available online at [www.sciencedirect.com](http://www.sciencedirect.com)

SCIENCE @ DIRECT®

Neural Networks xx (2005) 1–9

Neural  
Networks[www.elsevier.com/locate/neunet](http://www.elsevier.com/locate/neunet)

2005 Special issue

# A model of STDP based on spatially and temporally local information: Derivation and combination with gated decay<sup>☆</sup>

Anatoli Gorchetchnikov<sup>a,\*</sup>, Massimiliano Versace<sup>a</sup>, Michael E. Hasselmo<sup>b</sup><sup>a</sup>Department of Cognitive and Neural Systems, Boston University, 677 Beacon St, Boston, MA 02215, USA<sup>b</sup>Department of Psychology, Boston University, 64 Cummington St, Boston, MA 02215, USA

## Abstract

Temporal relationships between neuronal firing and plasticity have received significant attention in recent decades. Neurophysiological studies have shown the phenomenon of spike-timing-dependent plasticity (STDP). Various models were suggested to implement an STDP-like learning rule in artificial networks based on spiking neuronal representations. The rule presented here was developed under three constraints. First, it only depends on the information that is available at the synapse at the time of synaptic modification. Second, it naturally follows from neurophysiological and psychological research starting with Hebb's postulate [D. Hebb. (1949). *The organization of behavior*. Wiley, New York]. Third, it is simple, computationally cheap and its parameters are straightforward to determine. This rule is further extended by addition of four different types of gating derived from conventionally used types of gated decay in learning rules for continuous firing rate neural networks. The results show that the advantages of using these gatings are transferred to the new rule without sacrificing its dependency on spike-timing.

© 2005 Published by Elsevier Ltd.

**Keywords:** Spike-timing-dependent plasticity; Gated decay; Learning rules; Spiking neural networks

Most neural models have focused on the Hebb rule for synaptic plasticity, which can be written as:

$$\frac{dw}{dt} = \lambda X_{\text{pre}} X_{\text{post}} \quad (1)$$

where  $\lambda$  is the learning rate and  $X$  are pre- and postsynaptic signals. This formula is based on correlation and does not include precise information about firing times of neurons, unless  $X_{\text{pre}}$  and  $X_{\text{post}}$  are specifically designed to include this information. Hebb (1949), on the other hand, emphasized causality and, therefore, a temporal order of neuronal firing.

Moreover, neurophysiological studies have focused on temporal relationships of neuronal firing and plasticity and explored the phenomenon of spike-timing-dependent plasticity (STDP) (Bi & Poo, 2001; Levy & Steward, 1983; Markram, Lubk, Frotscher, & Sakmann, 1997). STDP

manifests itself in potentiation of the synapse if the presynaptic spike precedes the postsynaptic spike, and in depression if the presynaptic spike follows the postsynaptic spike. STDP more closely reflects the idea of the Hebbian postulate than Eq. (1). Various implementations of learning rules that can model this type of plasticity were proposed in recent years (Gerstner, Kempter, van Hemmen, & Wagner, 1999, Chapter 14; Kepecsvan, Rossum, Song, & Tegner, 2002; Porr, Saudargiene, & Wörgötter, 2004; Song, Miller, & Abbott, 2000).

The model presented here also assumes that the adaptation is based on temporally asymmetric adjustment of projection weights, and develops the mechanism to implement STDP on the basis of information available in the synapse at the moment of learning. The brief version of this research was presented at the International Joint Conference on Neural Networks (Gorchetchnikov, Versace, & Hasselmo, 2005). Here we extend the reasoning behind the mathematics and design decisions that were made to construct our model of spike-timing-dependent plasticity. This model uses Eq. (1) and designs  $X_{\text{pre}}$  and  $X_{\text{post}}$  so that the resulting rule shows the features of experimentally recorded STDP. This rule can be integrated over time to achieve results similar to those produced by a well studied rule suggested by Gerstner et al. (1999), which is discussed in the next section.

<sup>☆</sup> An abbreviated version of some portions of this article appeared in Gorchetchnikov, Versace, and Hasselmo (2005), as part of the IJCNN 2005 conference proceedings, published under the IEEE copyright.

\* Corresponding author. Tel.: +1 617 353 1433.

E-mail addresses: [anatoli@cns.bu.edu](mailto:anatoli@cns.bu.edu) (A. Gorchetchnikov), [versace@cns.bu.edu](mailto:versace@cns.bu.edu) (M. Versace), [hasselmo@bu.edu](mailto:hasselmo@bu.edu) (M.E. Hasselmo).

## 1. Previous analysis and notation

Gerstner et al. (1999) analyzed the following STDP rule:

$$\Delta w_{ij} = \int_0^T \int_0^T W(t-t') S_i(t) S_j(t') dt dt' \quad (2)$$

where  $w_{ij}$  is the synaptic weight of a connection from  $j$  to  $i$ ,  $T$  is the duration of a learning experiment,  $S_i(t)$  is the postsynaptic spike train,  $S_j(t)$  is the presynaptic spike train, and  $W(t-t')$  is the learning window that depends on the time difference between the postsynaptic  $t$  and presynaptic  $t'$  spikes and is described as

$$W(s) = \begin{cases} [A_+ - A_-] e^{-(s-s^*)/\tau} & \text{for } s > s^* \\ A_+ e^{-(s-s^*)/\tau_+} - A_- e^{-(s-s^*)/\tau_-} & \text{for } s < s^* \end{cases} \quad (3)$$

where  $A_+$ ,  $A_-$ ,  $t_+$ ,  $t_-$  are parameters defining the shape of the window,  $\tau$  is the synaptic time constant, and  $s^*$  determines the time difference corresponding to the peak of potentiation. Note, that Gerstner et al. (1999) used  $s = t' - t$ , so the respective signs are flipped in the above equations.

Eq. (2) contains the information about timing of the presynaptic spike arrival, timing of the postsynaptic spike generation, and efficiency of learning for a specific time difference between the two. These are the three critical components that have to be present in any STDP rule. The rule (2) has several advantages. First, it is spatially local in the sense that it does not require any information that is not available at the synapse the rule is applied to. Second, the number of parameters in the learning window provides enough flexibility to fit any experimental data. Finally, it reduces to Hebbian learning for the continuous firing rate coding (Gerstner et al., 1999).

The downside of this rule is its requirement for the timing information over the interval  $[0, T]$ , so it is temporally global. Efficient simulation software will prefer a temporally local rule based only on the information available here and now over the one that requires keeping track of recent events.

## 2. Components of a temporally and spatially local STDP rule

To create a temporally and spatially local STDP rule one should identify three components of the plasticity, namely presynaptic timing, postsynaptic timing, and the efficiency of learning for a certain time difference, so that all of them are available at the synapse at every moment of time.

Levy and Steward (1983) suggested that the accumulation of calcium ions in the spine can indicate recent presynaptic spiking. A related indicator of presynaptic spike timing at the site of the synapse is the synaptic conductance. It has a temporal profile, which is triggered by a presynaptic spike and approximated here by a dual-exponential equation.

Retrograde electrical invasion was suggested by Levy and Steward (1983) to subserve the indication of postsynaptic spike timing. The model presented here uses the membrane potential directly. Moreover, since the model assumes that 0 is the resting potential, and the time of the spike is the moment when potential crosses 0 between the depolarization part of the spike and the afterhyperpolarization (AHP), membrane potential is positive before the spike and negative after the spike. This can be used to determine the efficiency of learning.

The efficiency of learning at every moment of time is the slice of the learning window  $W$  in Eq. (3). Gerstner et al. (1999) description of the formation of such a window is based on two factors. The first ( $a$ ) is triggered by the presynaptic spike. The second ( $b$ ) is triggered by the postsynaptic spike and can have potentiation and depression components ( $b_+$  and  $b_-$ , respectively). This discussion applies here if one considers synaptic conductance as an  $a$  factor (which is always positive), and membrane potential as a sum of positive (depolarization)  $b_+$  and negative (AHP)  $b_-$  components.

Biophysically, all three components of STDP might follow from a single mechanism, for example Holmes and Levy (1990) conducted a detailed quantitative study of  $\text{Ca}^{++}$  accumulation in the dendritic spine and its relation to the long-term potentiation (LTP). Their results suggest that  $\text{Ca}^{++}$  dynamics in the spine can monitor both pre- and postsynaptic signals, and the time course of these dynamics affects the learning window. The model presented here is more abstract and monitors pre- and postsynaptic signals separately.

Substituting synaptic conductance as a presynaptic signal ( $X_{\text{pre}} = g_s$ ) and membrane potential as a postsynaptic signal ( $X_{\text{post}} = V_{\text{soma}}$ ) in Eq. (1) can produce STDP due to the mechanism discussed by Gorchetchnikov and Hasselmo (in press). A similar idea was used by Porr et al. (2004), but the authors use the derivative of the back-propagating action potential as  $X_{\text{post}}$ . Numerical simulations (Gorchetchnikov & Hasselmo, in press) generally confirmed the approach to the STDP rule presented here, but the formal analysis of a simplified version can provide additional insights on the dynamics of this rule.

## 3. Analysis of the simplified rule

The following simplifications were made for the analysis:

**Simplification 1:** Approximate the effect of presynaptic transmitter release on synaptic conductance by an alpha function:

$$g_s = \bar{g}_s \frac{t}{\tau} e^{-(t/\tau)} \quad (4)$$

where  $\bar{g}_s$  is the maximal channel conductance,  $t$  is the time since the presynaptic action potential, and  $\tau$  is the time

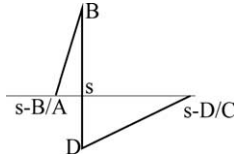


Fig. 1. Approximation of the action potential with a piecewise linear function.

constant of the channel. Additionally, assume that it starts at  $t=0$  (and therefore  $s=t_{\text{post}}$ ) and completely decays at  $t=10\tau$ .

**Simplification 2:** Approximate the postsynaptic action potential with a piecewise linear function

$$X_{\text{post}} = \begin{cases} A(t-s) + B & \text{if } s - \frac{B}{A} < t \leq s \\ C(t-s) + D & \text{if } s < t < s - \frac{D}{C} \\ 0 & \text{otherwise} \end{cases} \quad (5)$$

as shown in Fig. 1:  $X_{\text{post}} = A(t-s) + B$  models the depolarization part, where  $A > 0$  is the slope of a spike and  $B > 0$  is a peak amplitude, and  $X_{\text{post}} = C(t-s) + D$  models the hyperpolarization part, where  $C > 0$  is the slope and  $D < 0$  is the trough amplitude.

Then the rule (1) becomes

$$\frac{dw}{dt} = \begin{cases} (A(t-s) + B) \frac{t}{\tau} e^{(1-t/\tau)} & \text{if } s - \frac{B}{A} < t \leq s \\ (C(t-s) + D) \frac{t}{\tau} e^{(1-t/\tau)} & \text{if } s < t < s - \frac{D}{C} \end{cases} \quad (6)$$

With the above simplifications learning only happens if  $(D/C) < s < 10\tau + (B/A)$  as illustrated in Fig. 2.

To estimate the total weight change during one learning window, Eq. (6) has to be integrated over the length of the learning window. This integral has an analytic solution

$$-e^{(1-t/\tau)}((v - \mu s)(t + \tau) + \mu(t + \tau)^2 + \mu\tau^2) + X \quad (7)$$

where  $\mu = A$ ,  $v = B$  for  $s - (B/A) < t \leq s$ , and  $\mu = C$ ,  $v = D$  for  $s < t < s - (D/C)$ . Separating these two cases, one can denote part of this solution for potentiation while  $s - (B/A) < t \leq s$  as  $\Phi_P$ , and for depression while  $s < t < s - (D/C)$  as  $\Phi_D$ . The total weight change is

$$\Delta w = \Phi_P \Big|_{t_1}^{t_2} + \Phi_D \Big|_{t_2}^{t_3} \quad (8)$$

The limits of integration are determined as follows.

*Case 1:* if  $(D/C) < s < 0$ , then  $\Phi_P = 0$ ,  $\Phi_D$  starts at  $t=0$  and lasts till either  $t=s - (D/C)$  or  $t=10\tau$ , whichever comes first.

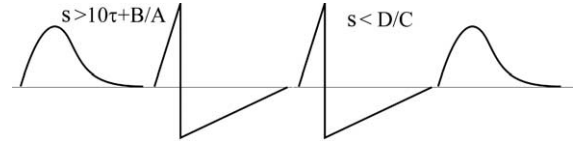
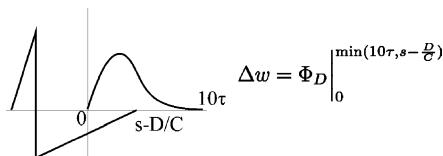
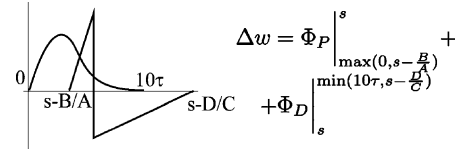
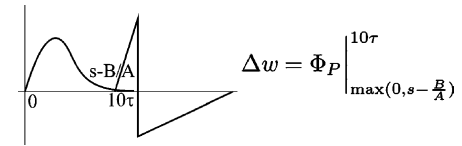


Fig. 2. Cases with no learning after simplifications.

*Case 2:* if  $0 < s < 10\tau$ , then  $\Phi_P$  starts at either  $t=s - (B/A)$  or  $t=0$ , whichever comes last, and lasts till  $t=s$ .  $\Phi_D$  starts at  $t=s$  and lasts till either  $t=s - (D/C)$  or  $t=10\tau$ , whichever comes first.



*Case 3:* if  $10\tau < s < 10\tau + (B/A)$ , then  $\Phi_D = 0$ ,  $\Phi_P$  starts at either  $t=s - (B/A)$  or  $t=0$ , whichever comes last and lasts till  $t=10\tau$ .



Combining all cases yields:

$$\Delta w = \Phi_P \Big|_{\max(0, s - (B/A))}^{\max(0, \min(s, 10\tau))} + \Phi_D \Big|_{\max(s, 0)}^{\max(s, \min(10\tau, s - (D/C)))} \quad (9)$$

Fig. 3 plots Eq. (9) and shows the contribution of potentiation and depression components.

Determining the precise timing differences  $s$  of peak potentiation and trough depression is nontrivial, because in

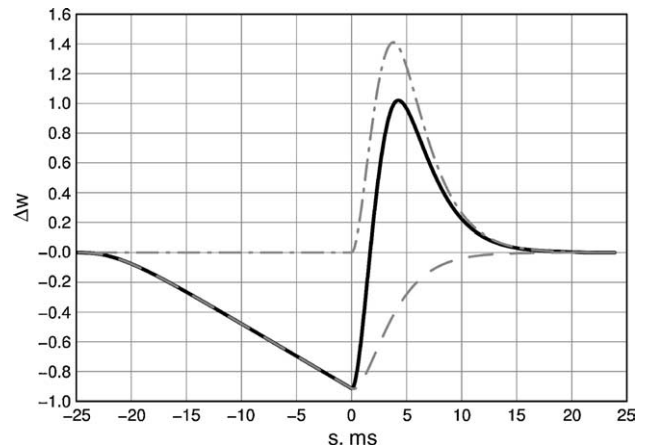


Fig. 3. Example plot of STDP curve for a simplified rule with normalized parameters.  $\Phi_P$  is shown by dot-dashed line,  $\Phi_D$  is represented by long-dashed line, and their sum Eq. (9) is shown as bold black line.  $A=0.2$ ,  $B=0.8$ ,  $C=0.008$ ,  $D=-0.2$ , and  $\tau=2$  ms.

some cases taking the derivative of the Eq. (9) leads to transcendent equations, which are analytically unsolvable. The parameter manipulations suggest that the increase of either slope  $A$  or  $C$  shifts the respective peaks towards  $\tau$ . Decrease of the slope  $C$  for hyperpolarization shifts the depression trough towards  $s=0$ . Decrease of the slope  $A$  for depolarization shifts the peak potentiation towards  $s \approx e \ln(B/A)$ .

The parameter choice for the plot in Fig. 3 leads to overall depression greater than the overall potentiation. Analysis has shown that this is the necessary condition to assure that uncorrelated inputs lead to depression (Song et al., 2000) and to make the learning process stable (Kepecs et al., 2002).

#### 4. Limiting the weights

Eq. (9) was derived directly from the Hebbian rule, therefore it inherits the major drawback of Eq. (1), namely the resulting synaptic weights can grow infinitely large. There are several approaches to prevent such an unbounded weight growth in the Hebbian rule:

- Renormalizing the weights to keep the total weight constant;
- Imposing a limit on the weight value;
- Adding to Eq. (1) the decay term proportional to the current weight value.

Renormalizing the weights is not considered here, because it requires information from all synapses for the calculation, and, therefore, violates the spatial locality requirement for the rule.

Limits on the weight value can be hard or soft. With hard bounds on each step of calculation the weight is checked against the interval of allowed values. In case the weight is outside of this interval, it is set to the value of the nearest end of the interval. Soft limits use the difference between the current weight and the bound as a factor in the rule

$$\frac{dw}{dt} = \lambda X_{\text{pre}} X_{\text{post}} (w - w_{\text{MIN}})(w_{\text{MAX}} - w) \quad (10)$$

In this case where the weight approaches one of the bounds, the change becomes smaller, since the respective difference goes to zero. With  $t \rightarrow \infty$ , the weight will approach either  $w_{\text{MAX}}$  or  $w_{\text{MIN}}$ . Such a bimodal distribution means strong competition and rate stabilization (Kepecs et al., 2002), but it does not preserve the relative importance of input cells for the firing of the output cell, and therefore disregards the causality emphasized by Hebb (1949). In other words the postsynaptic cell cannot learn the spatio-temporal pattern of inputs (Grossberg, 1974).

If only depression or only potentiation depends on the difference between the respective bound and the current

Table 1  
Gated decay for continuous firing rate representations

Common name	$f(X_{\text{pre}}, X_{\text{post}})$	$\lim_{t \rightarrow \infty} w$
Grossberg outstar (Grossberg, 1974; 1976a,b) or postsynaptically gated decay	$X_{\text{post}}$	$X_{\text{pre}}$
Grossberg instar (Grossberg, 1974; 1976a,b) or presynaptically gated decay	$X_{\text{pre}}$	$X_{\text{post}}$
Oja rule (Oja, 1982)	$X_{\text{post}}^2$	$X_{\text{pre}}/X_{\text{post}}$

weight, the distribution of resulting weights is unimodal. A unimodal distribution leads to principal component extraction and preserves the total weight (Kepecs et al., 2002). These are desirable goals, but in the case of Eq. (10), removal of either bound would mean an unlimited weight change in the respective direction.

Another way to achieve pattern sampling that extracts the relative importance of the inputs for the firing of the postsynaptic cell is to introduce a decay term proportional to the current weight. Grossberg introduced the postsynaptic and presynaptic gated decay laws and called them the Instar and Outstar learning rules (Grossberg, 1974, 1976a,b). Such a decay leads to the rule

$$\frac{dw}{dt} = \lambda X_{\text{pre}} X_{\text{post}} - f(X_{\text{pre}}, X_{\text{post}}) w \quad (11)$$

where  $f(X_{\text{pre}}, X_{\text{post}})$  is a scaling function. Some scaling functions that are widely used with continuous firing rate neuronal representations are listed in Table 1. According to Abbott and Nelson (2000), the experimental data suggests that  $f$  must be positive or negative depending on the postsynaptic rate. Mathematically this suggestion is perfectly sound, but biophysically the case of negative  $f$  means a non-Hebbian weight increase in addition to STDP.

All functions listed in Table 1 only make sense when one considers pre- and postsynaptic signals as firing rates. In this case the firing patterns of cells have only a spatial component. A temporal component is hinted at by the firing rate of the cell, which is coded as the level of activity. Therefore, when the  $\lim_{t \rightarrow \infty} w$  converges to the level of activity of the presynaptic or postsynaptic cell, it provides a good representation of the spatial pattern. In the case of spiking neurons, the temporal component of the pattern is fully represented by a specific time difference between the presynaptic and the postsynaptic spike. Hence, the  $\lim_{t \rightarrow \infty} w$  should somehow represent this time difference. Section 5 starts the design of a scaling function  $f$  applicable for spiking networks.

#### 5. Combining gated decay and the STDP rule

Rule (6) provides the measure of the time difference between the presynaptic and postsynaptic spike based on the product of  $X_{\text{pre}}$  and  $X_{\text{post}}$ . The successful learning rule for spiking neurons can sample some function  $q$  of this product



in order to encode both spatial and temporal components of the pattern. To achieve this, the rule should lead to

$$\lim_{t \rightarrow \infty} w = q(X_{\text{pre}} X_{\text{post}}) \quad (12)$$

From a biophysical point of view, the synaptic weight can not be negative if it is defined as a density of the ion channels in the synapse. To satisfy this constraint  $q(X_{\text{pre}}, X_{\text{post}})$  should be non-negative in Eq. (12). While  $X_{\text{pre}} = g_s \in [0, 1]$ ,  $X_{\text{post}} = V_{\text{soma}}$  can be both positive and negative. Moreover, the bounds of  $X_{\text{post}}$  can be only approximated from the data on membrane potential.

To overcome the problem of loosely defined bounds,  $X_{\text{post}}$  can be replaced by a variable triggered by membrane potential but bounded within a certain interval. This is done by setting the parameters A, B, C, and D of Eq. (5) to normalize the values of  $X_{\text{post}}$  over the interval  $[D, B]$  of the length 1.

The piecewise linear  $X_{\text{post}}$  used in Fig. 3 changes between  $D < 0$  and  $B > 0$ . Hence, the product  $X_{\text{pre}} X_{\text{post}} \in [D, B]$ , and since  $B - D = 1$

$$q(X_{\text{pre}} X_{\text{post}}) = X_{\text{pre}} X_{\text{post}} - D \in [0, 1] \quad (13)$$

This function  $q$  leads to following:

- $\lim_{t \rightarrow \infty} w = 1$  when  $X_{\text{pre}} X_{\text{post}} = B$  (positive correlation)
- $\lim_{t \rightarrow \infty} w = 0$  when  $X_{\text{pre}} X_{\text{post}} = D$  (negative correlation) and
- $\lim_{t \rightarrow \infty} w = -D$  when  $X_{\text{pre}} X_{\text{post}} = 0$  (no correlated activity between pre- and postsynaptic cells).

There are three issues with the Eq. (5) and the resulting STDP curve in Fig. 3. First, in general case the shape of the action potential during simulation will not follow the linear approximation used here. To keep the learning rule simple yet applicable with any spike shape the approximated  $X_{\text{post}}$  still can be used, but instead of precisely following the shape of the spike it should be triggered by action potential generation.

Second, for the case of spike-generating mechanisms that have internal dynamics (e.g. the classic [Hodgkin & Huxley, 1952](#) model), the length of the spike is not constant. To accommodate this, the positive part of  $X_{\text{post}}$  should be triggered by an instantaneous event that signals the generation of an action potential in the near future, and should last for the duration of the spike. The simplest function that satisfies these requirements and does not depend on the length of the spike is  $X_{\text{post}} = \text{constant}$  starting when  $V_{\text{soma}}$  crosses the spiking threshold and ending when  $V_{\text{soma}}$  drops below the resting potential after the spike.

The third problem is the shift of zero-crossing towards positive  $s$  in Fig. 3. It is due to the instantaneous effect of the emitted postsynaptic spike on synaptic modification in the model. In real cells there is a delay before the chemical and electrical influence of the action potential can back-propagate to the dendrites and reach the synapse. A delay in the transition from a positive to a negative component of  $X_{\text{post}}$  can correct the shift in zero-crossing. Moreover, from

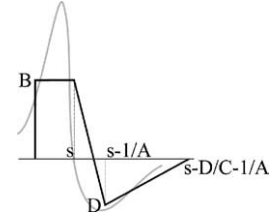


Fig. 4.  $X_{\text{post}}$  as piecewise linear function Eq. (14). The action potential represented by this  $X_{\text{post}}$  is outlined in gray in the background.

a biophysical standpoint this transition should be gradual and not instantaneous as was used in Eq. (5). Linear decay is sufficient as the first approximation. The resulting  $X_{\text{post}}$  is

$$X_{\text{post}} = \begin{cases} B & \text{if } V_{\text{soma}} > V\theta \\ A(t - s) + B & \text{if } s < t < s - \frac{1}{A} \\ C\left(t - s + \frac{1}{A}\right) + D & \text{if } s - \frac{1}{A} < t < s - \frac{D}{C} - \frac{1}{A} \\ 0 & \text{otherwise} \end{cases} \quad (14)$$

where  $A < 0$  (note the change of the sign from Eq. (5)) is the slope of a transition from a positive to a negative component,  $B > 0$  is the peak amplitude of a positive component,  $C > 0$  is the slope of recovery and  $D = B - 1 < 0$  is the trough amplitude of a negative component. Fig. 4 shows the resulting  $X_{\text{post}}$ .

Biophysically, this shape of  $X_{\text{post}}$  can be justified as follows. Crossing a certain voltage level (e.g. spiking threshold) opens  $Ca^{++}$  channels and causes some  $Ca^{++}$ -dependent metabolic process that underlies synaptic facilitation in the cell. After the action potential is emitted, the residual  $Ca^{++}$  concentration gradually wears off. At lower levels of  $Ca^{++}$  another metabolic process that underlies synaptic depression takes over. Finally, after  $Ca^{++}$  concentration returns to rest, the synaptic change stops. This reasoning is supported by the data showing that brief and high  $Ca^{++}$  concentrations lead to synaptic potentiation and longer and lower  $Ca^{++}$  concentrations lead to depression ([Yang Tang, & Zucker, 1999](#)). Note, that with proper choice of parameters in Eq. (14), the balance between potentiation and depression can be set so that the learning will produce depression or no change in the case of a single postsynaptic spike and potentiation in the case of a postsynaptic burst. This effect was reported in several preparations and reviewed by [Dan and Poo \(2004\)](#). In the model it is produced by lengthening the first component of the Eq. (14) by bursting activity relative to a single spike.

Mathematically, the new  $X_{\text{post}}$  adds an extra term to Eq. (8)

$$\Delta w = \Phi_P|_{t_1}^{t_2} + \Phi_T|_{t_2}^{t_3} + \Phi_D|_{t_3}^{t_4} \quad (15)$$

where  $\Phi_D$  is a depression component similar to the one discussed for Eq. (8) and calculated using Eq. (7),  $\Phi_T$  is

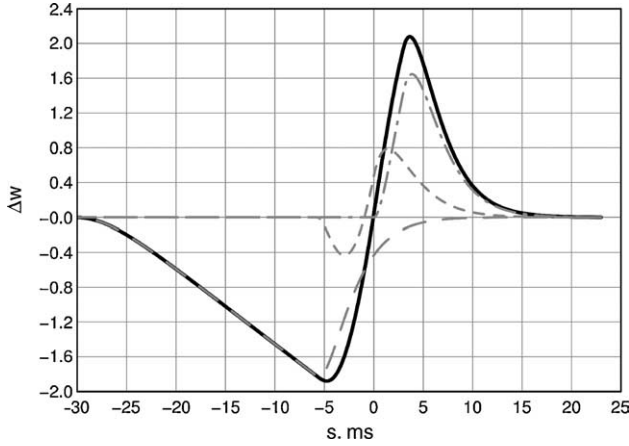


Fig. 5. Example plot of STDP curve for an extended rule.  $\Phi_P$  is shown as dot-dashed line,  $\Phi_D$  as long-dashed line,  $\Phi_T$  as short-dashed line, and their sum (Eq. 15) as bold black line.  $A = -0.175$ ,  $B = 0.6$ ,  $C = 0.016$ ,  $D = B - 1 = -0.4$ ,  $t^* = s - 3$  ms, and  $\tau = 2$  ms.

a transition component also calculated using Eq. (7), and  $\Phi_P$  is a potentiation component calculated as

$$\begin{aligned} \Phi_P|_{t_1}^{t_2} &= \int_{t_1}^{t_2} B \frac{t}{\tau} e^{(1-(t/\tau))} dt \\ &= -e^{(1-(t/\tau))} B(t + \tau) \Big|_{\min(\max(0, t^*), s)}^{\max(t^*, \min(s, 10\tau))} \end{aligned} \quad (16)$$

where  $t^*$  is the time when  $V_{\text{soma}}$  crosses the threshold. The result of Eq. (15) is presented in Fig. 5.

As a result of these adjustments, the target of the learning rule becomes

$$\lim_{t \rightarrow \infty} w = q(X_{\text{pre}}X_{\text{post}}) = X_{\text{pre}}X_{\text{post}} + 1 - B \quad (17)$$

with three free parameters:  $A < 0$ ,  $0 < B < 1$ , and  $C > 0$ . Eq. (17) keeps the resulting weights in the interval  $[0, 1]$ .

### 6. Extending the interval for synaptic weights

The regular procedure to extend the range of  $q(X_{\text{pre}}X_{\text{post}})$  over  $[\check{w}, \hat{w}]$  is to multiply it by the length of the interval and add  $\check{w}$

$$q(X_{\text{pre}}X_{\text{post}}) = (X_{\text{pre}}X_{\text{post}} + 1 - B)(\hat{w} - \check{w}) + \check{w} \quad (18)$$

Similar to Eq. (13) it can be shown that  $\lim_{t \rightarrow \infty} w = \hat{w}$  when  $X_{\text{pre}}X_{\text{post}} = B$ , and  $\lim_{t \rightarrow \infty} w = \check{w}$  when  $X_{\text{pre}}X_{\text{post}} = 1 - B$ .

In the case where  $X_{\text{pre}}X_{\text{post}} = 0$

$$\lim_{t \rightarrow \infty} w = \hat{w} - B(\hat{w} - \check{w}) = w_0 \quad (19)$$

where  $w_0$  stands for the baseline weight achieved when there is no correlation between presynaptic and postsynaptic firing. Rewriting the parameter  $B$  in terms of maximal, minimal and baseline weights and substituting it in the Eq. (18) yields

$$\lim_{t \rightarrow \infty} w = q(X_{\text{pre}}X_{\text{post}}) = X_{\text{pre}}X_{\text{post}}(\hat{w} - \check{w}) + w_0 \quad (20)$$

To achieve this limit, the differential equation for the weight should be

$$\frac{dw}{dt} = \lambda(X_{\text{pre}}X_{\text{post}}(\hat{w} - \check{w}) + w_0 - w) \quad (21)$$

which suggests in comparison with Eq. (11) that for spiking neurons a reasonable scaling function is  $f(X_{\text{pre}}X_{\text{post}}) = \lambda$ . Unfortunately, this scaling function was shown to force the weights towards the baseline since the events of pre- and postsynaptic coactivity are quite rare and the drive towards the baseline is constant (Grossberg, 1974).

The solution for continuous firing rate neurons was to gate the decay by either pre- or postsynaptic activity. But gating the decay term alone would change the limit in Eq. (12) and, therefore, invalidate the reasoning of the previous two sections. The solution suggested here is to gate not the decay term but the whole learning process of Eq. (21) by either presynaptic, or postsynaptic, or both activities (for an example of such a dual gating during visual perceptual learning see Grossberg, Hwang, & Mingolla, 2002). The resulting rule becomes

$$\frac{dw}{dt} = \lambda(X_{\text{pre}}X_{\text{post}}(\hat{w} - \check{w}) + w_0 - w)f_G(X_{\text{pre}}X_{\text{post}}) \quad (22)$$

where  $f_G$  is a gating function. The only requirement that this gating function has to satisfy is non-negativity ( $f_G \geq 0$ ), so that it does not affect the sign of the weight change determined by the interaction of the presynaptic and postsynaptic signal. The next section discusses the results for five different gating functions.

### 7. Comparison of five gating functions

The simulations presented in this section used the network of three fully interconnected cells named A, B, and C as shown in Fig. 6. Cells A and B were spiking so that cell B was lagging behind cell A by 10 ms, and cell C was always silent. The pair of spikes in cells A and B constitutes a learning trial. These trials were repeated every 200 ms, and over the total length of the simulation (1 s) there were five trials. This was sufficient for the weights to get within 1% of their asymptotes under all but the last gating function described below. For the last gating function the total length of the simulation was 5 s and included 25 learning trials. Parameters in these simulation were:  $\check{w} = 0$ ,  $\hat{w} = 5$ ,  $w_0 = 0.5$ ,

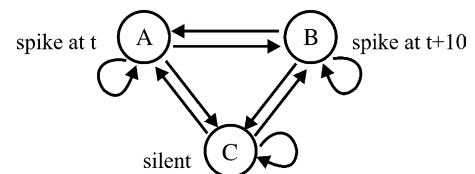


Fig. 6. The network used for testing gating functions.

Table 2  
Initial weights in the study of gating functions

Postsynaptic cell	Presynaptic cell		
	A	B	C
A	1.278943	3.706319	1.975214
B	3.632909	4.055134	3.862882
C	0.659782	4.121144	3.365119

and  $\lambda=1$ . All simulations started with random weights between cells presented in Table 2 that were drawn from a uniform distribution between  $\check{w}$  and  $\hat{w}$ .

In the simplest case there is no gating

$$f_G(X_{pre}, X_{post}) = \text{const} \quad (23)$$

and the weight decays exponentially all the time. Since spikes are relatively rare events,  $X_{pre}X_{post}=0$  most of the time, and the weight decays to  $w_0$  so fast, that the timing of pre- and postsynaptic spikes has a very small effect on the resulting weights as shown in Table 3. The constant in Eq. (23) was set as  $\text{const}=0.04$ .

While the magnitude of the deviation of resulting weights from  $w_0$  is too small to be usable, the sign of this deviation is correct. For the cases when the presynaptic spike follows the postsynaptic spike (A–A, B–B, and B–A) the weights settle to the value below  $w_0$ , while for the case A–B when the presynaptic spike precedes the postsynaptic spike, the weight settles to a value greater than  $w_0$ .

Assuming that in an attempt to learn the correlation of activities of two cells one can safely ignore intervals when both of the activities are zero, the first gating function studied here is

$$f_G(X_{pre}, X_{post}) = aX_{pre} + bX_{post}^2 \quad (24)$$

where  $a$  and  $b$  are positive coefficients, and the square is used to make the second term nonnegative. In this case the decay only happens during the nonzero signal in either the presynaptic or postsynaptic cell. This type of gating is termed *dual OR gating* henceforth. The results for this function with  $a=b=2$  are presented in Table 4. Since cell C is silent, there is no change in the strength of its projection to itself ( $f_G=0$  throughout the simulation; weights italicized in the table). A comparison of these results with the results for no gating shows that the deviations of the resulting weights were amplified by more than an order of magnitude, while the pattern of these weights was preserved for active cells.

Table 3  
Resulting weights with no gating

Postsynaptic cell	Presynaptic cell		
	A	B	C
A	0.499858	0.499484	0.5
B	0.505287	0.499787	0.5
C	0.5	0.5	0.5

Table 4  
Resulting weights with dual OR gating

Postsynaptic cell	Presynaptic cell		
	A	B	C
A	0.424987	0.455724	0.5
B	0.750113	0.423737	0.5
C	0.5	0.5	<i>3.365119</i>

Presynaptic gating is defined as

$$f_G(X_{pre}, X_{post}) = aX_{pre} \quad (25)$$

where  $a$  is a positive coefficient. The results for this function with  $a=2$  are presented in Table 5. Presynaptic gating leads to even better separation of learned weights than dual OR gating. In addition to this, it leaves all projections from a silent cell intact (italicized).

Postsynaptic gating is defined as

$$f_G(X_{pre}, X_{post}) = bX_{post}^2 \quad (26)$$

where  $b$  is a positive coefficient, and the square is used to make the gating nonnegative. The results for this function with  $b=2$  are presented in Table 6.

While presynaptic gating prevents modification of the outgoing projections from a silent cell, postsynaptic gating leaves incoming projections to a silent cell intact (italicized). The increase of the A to B weight is less prominent than with presynaptic gating, but better than with dual OR gating. Unlike the previous three cases, A to A and B to B projection weights do not decrease below  $w_0$  with the postsynaptic gating, and the B to A weight decreases only slightly below  $w_0$ . The reason for these results is investigated in the next section.

Finally, one can restrict the decay even further, and require that it only happens during the learning window, when  $X_{pre}X_{post} \neq 0$ . This leads to *dual AND gating*:

$$f_G(X_{pre}, X_{post}) = cX_{pre}X_{post}^2 \quad (27)$$

Table 5  
Resulting weights with presynaptic gating

Postsynaptic cell	Presynaptic cell		
	A	B	C
A	0.419419	0.455241	<i>1.975214</i>
B	1.201898	0.418226	<i>3.862882</i>
C	0.5	0.5	<i>3.365119</i>

Table 6  
Resulting weights with postsynaptic gating

Postsynaptic cell	Presynaptic cell		
	A	B	C
A	0.568417	0.489494	0.5
B	1.026381	0.569432	0.5
C	<i>0.659782</i>	<i>4.121144</i>	<i>3.365119</i>

Table 7  
Resulting weights with dual AND gating

Postsynaptic cell	Presynaptic cell		
	A	B	C
A	0.763313**	0.301894	1.975214
B	1.191229*	0.761404**	3.862882
C	0.659782	4.121144	3.365119

\* Reached asymptote after 1 s of stimulation.  
\*\* Reached asymptote at 5 s.

where  $c$  is a positive coefficient, and the square is used to make the gating nonnegative. The results for this function with  $c = 10$  are presented in Table 7.

This approach is the least intrusive, it only reshapes the pattern of weights when cells on both ends of projection are active. Projections to and from a silent cell do not change (italicized). The only role of decay here is to enforce Eq. (20). Since the learning is so restricted, it takes longer for the weights to reach their asymptotes than in the previous four cases. One value of the weight (marked with asterisk) reached the asymptote after 1 s of the simulation. Values marked with a double asterisk reached the asymptote at 5 s. Dual AND gating showed the best separation between A to B and B to A weights, but it also inherited from postsynaptic gating and amplified the problem with A to A and B to B projections. Since this problem can stem from the different shapes of STDP curves for these gating functions, the next section compares these curves for all five functions.

### 8. STDP curves for five gating functions

Addition of gatings to the learning rule and transition from Eqs. (21) and (22) makes the resulting equation impossible to integrate analytically. Instead of calculating the shape of STDP curve as was done in previous subsections, here these curves were built using simulations. In these simulations the time interval between the presynaptic and the postsynaptic spike varied on the interval  $[-30,30]$  ms. Trial setup was the same as in the previous section. Parameters for the  $X_{\text{post}}$  approximation were:  $A = -0.175$  and  $C = 0.02$ .  $B = 0.5$  and  $D = -0.5$  were calculated through  $\tilde{w} = 0$ ,  $\hat{w} = 2$ , and  $w_0 = 1$ . Learning rate was set to  $\lambda = 1$ ; all coefficients in Eqs. (24)–(27) were set to 1. All simulations started with initial weights equal to  $w_0 = 1$ . Cells in these simulations had axons with 3 ms delay, and the timing of the presynaptic spike was recorded at the soma. Since the effects of these spikes only manifested themselves 3 ms later, all plots appear shifted to the right. The actual arrival of the presynaptic spike to the axonal terminal is marked in Fig. 7 with a vertical dashed line.

The results are plotted in Fig. 7. All STDP curves follow a general trend for the amplitude of weight change shown in the previous section. Additionally, these plots show that postsynaptic gating introduces asymmetry in the learning, where the depression is favored over the potentiation. This asymmetry is also present with dual OR gating, but not with dual AND gating, which suggests that it is caused by the enhanced depression during the time when the postsynaptic signal is present, while the presynaptic signal

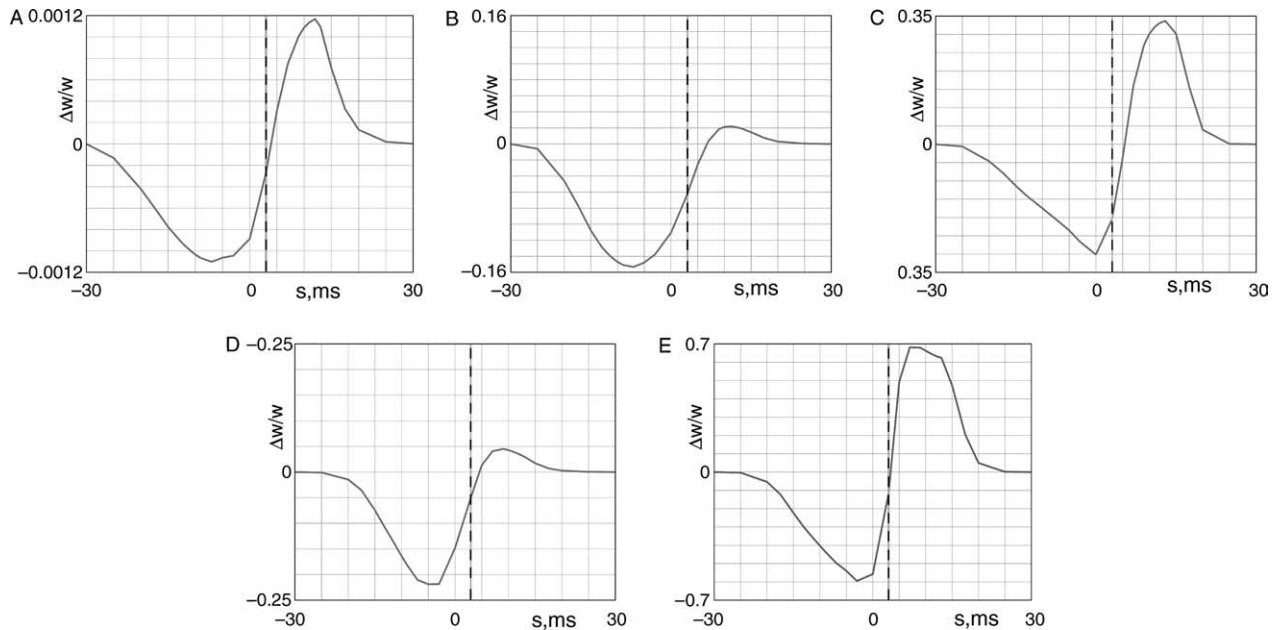


Fig. 7. STDP curves for five gating functions. A: No gating. Note the small amplitude of the resulting curve. B: Dual OR gating. Note the nonproportional increase in the depression amplitude. C: Presynaptic gating. D: Postsynaptic gating. E: Dual AND gating. Vertical dashed line shows the actual time when the presynaptic spike arrives at the axonal terminal.



is absent. Note that relative magnitudes of potentiation and depression can be manipulated through the parameter settings. In the simulations presented here  $w_0 - \check{w} = \hat{w} - w_0$ . Setting  $7(w_0 - \check{w}) = \hat{w} - w_0$  will lead to equal magnitudes of potentiation and depression for postsynaptic and dual OR gating, but will favor potentiation over depression for other types of gating.

Precise comparison of the relative shapes of these curves (see Gorchetchnikov, Versace, & Hasselmo, 2005) shows that on the depression part of the curve the dual OR gating is the closest in shape to the non-gated learning. The postsynaptic, dual AND, and presynaptic gatings are, respectively, shifting the peak depression further and further towards 0.

On the potentiation part of the curve, postsynaptic gating is the closest resembling the non-gated learning. Dual OR, postsynaptic, and dual AND gatings progressively shift the peak potentiation towards 0 (Gorchetchnikov et al., 2005). Postsynaptic and dual AND gatings have the two leftmost zero-crossings, which can account for the weights from a cell to itself settling to the values above  $w_0$  as was shown in the previous section.

## 9. Discussion

The rule (22) suggested here follows the general requirements for STDP and easily accommodates gating functions used in learning rules for continuous firing rate neuronal representations. Aside from setting the learning rate  $\lambda$ , the weight interval  $[\check{w}, \hat{w}]$ , and a baseline weight  $w_0$ , this rule only has two free parameters: a slope of transition from potentiation to depression  $A$  and a slope of depression  $C$ . Both of these slopes can be calculated through durations of the respective processes, which can be measured experimentally. Hence, we claim that parameters that the rule (22) uses are more intuitive and more appealing to experimental neuroscientists.

From the computational perspective, the rule presented here is simple and reliable. The analysis showed that by integration over a learning period this rule reduces to the equivalent of the well-described Gerstner et al. (1999) rule. Since the instantaneous weight change computed by Eq. (22) only depends on the locally available information at the specific moment of time, this change can be easily computed on-line during each integration step of the simulation. Moreover, this computation requires neither significant computational resources nor additional memory to store the information through time. We suggest it as a mechanism for instantaneous synaptic weight change in spiking neural networks.

## Acknowledgements

AG and MH were supported in part by NIH grants MH60013, MH61492, MH60450, and DA16454. MV was

supported in part by AFOSR F49620-01-1-0397 and ONR N00014-01-1-0624.

## References

- Abbott, L. F., & Nelson, S. B. (2000). Synaptic plasticity: Taming the beast. *Nature Neuroscience*, 3(suppl.), 1178–1183.
- Bi, G.-q., & Poo, M.-m. (2001). Synaptic modification by correlated activity: Hebb's postulate revisited. *Annual Review of Neuroscience*, 24, 139–166.
- Dan, Y., & Poo, M.-m. (2004). Spike timing-dependent plasticity of neural circuits. *Neuron*, 44, 23–30.
- Gerstner, W., Kempter, R., van Hemmen, J. L., & Wagner, H. (1999). Hebbian learning of pulse timing in the Barn Owl auditory system. In W. Maass, & C. M. Bishop (Eds.), *Pulsed neural networks* (pp. 353–377). Cambridge, MA: MIT Press, 353–377.
- Gorchetchnikov, A., & Hasselmo, M. E. (2005). A simple rule for spike-timing-dependent plasticity: Local influence of AHP current. [see also pages 885–890] *Neurocomputing*, 65–66, 885–890.
- Gorchetchnikov, A., Versace, M., & Hasselmo, M. E. (2005). Spatially and temporally local spike-timing-dependent plasticity rule. In *Proceedings of the International Joint Conference on Neural Networks*, Montreal, Canada, July 31–August 4.
- Grossberg, S. (1974). Classical and instrumental conditioning by neural networks. *Progress in Theoretical Biology*, 3, 51–141.
- Grossberg, S. (1976a). Adaptive pattern classification and universal recoding i: Parallel development and coding of neural feature detectors. *Biological Cybernetics*, 23, 121–134.
- Grossberg, S. (1976b). Adaptive pattern classification and universal recoding ii: Feedback, expectation, olfaction, and illusions. *Biological Cybernetics*, 23, 187–202.
- Grossberg, S., Hwang, S., & Mingolla, E. (2002). Thalamocortical dynamics of the McCollough effect: Boundary-surface alignment through perceptual learning. *Vision Research*, 42, 1259–1286.
- Hebb, D. (1949). *The organization of behavior*. New York: Wiley.
- Hodgkin, A. L., & Huxley, A. F. (1952). Quantitative description of membrane current and its application to conduction and excitation in nerve. *Journal of Physiology*, 117, 500–544.
- Holmes, W. R., & Levy, W. B. (1990). Insights into associative long-term potentiation from computational models of NMDA receptor-mediated calcium influx and intracellular calcium concentration changes. *Journal of Neurophysiology*, 63(5), 1148–1168.
- Kepecs, A., van Rossum, M. C. W., Song, S., & Tegner, J. (2002). Spike-timing-dependent plasticity: Common themes and divergent vistas. *Biological Cybernetics*, 87, 446–458.
- Levy, W. B., & Steward, O. (1983). Temporal contiguity requirements for long-term associative potentiation/depression in the hippocampus. *Neuroscience*, 8(4), 791–797.
- Markram, H., Lubke, J., Frotscher, M., & Sakmann, B. (1997). Regulation of synaptic efficacy by coincidence of postsynaptic APs and EPSPs. *Science*, 275, 213–215.
- Oja, E. (1982). A simplified neuron model as a principal component analyzer. *Journal of Mathematical Biology*, 15, 267–273.
- Porr, B., Saudargiene, A., & Wörgötter, F. (2004). Analytical solution of spike-timing dependent plasticity based on synaptic biophysics. In S. Thrun, L. Saul, & B. Schölkopf, *Advances in neural information processing systems* (16). Cambridge, MA: MIT Press.
- Song, S., Miller, K. D., & Abbott, L. F. (2000). Competitive Hebbian learning through spike-timing-dependent synaptic plasticity. *Nature Neuroscience*, 3, 919–926.
- Yang, S.-N., Tang, Y.-G., & Zucker, R. S. (1999). Selective induction of LTP and LTD by postsynaptic  $[Ca^{2+}]_i$  elevation. *Journal of Neurophysiology*, 81(2), 781–787.